(10)

Eighth Symposium

# NAVAL HYDRODYNAMICS

## HYDRODYNAMICS IN THE OCEAN ENVIRONMENT

ARC-179

Office of Naval Research
Department of the Navy

# UNSTEADY, FREE SURFACE FLOWS; SOLUTIONS EMPLOYING THE LAGRANGIAN DESCRIPTION OF THE MOTION

Christopher Brennen, Arthur K. Whitney
*California Institute of Technology*
*Pasadena, California*

ABSTRACT

Numerical techniques for the solution of unsteady free surface flows are briefly reviewed and consideration is given to the feasibility of methods involving parametric planes where the position and shape of the free surface are known in advance. A method for inviscid flows which uses the Lagrangian description of the motion is developed. This exploits the flexibility in the choice of Lagrangian reference coordinates and is readily adapted to include terms due to inhomogeneity of the fluid. Numerical results are compared in two cases of irrotational flow of a homogeneous fluid for which Lagrangian linearized solutions can be constructed. Some examples of wave run-up on a beach and a shelf are then computed.

## I. INTRODUCTION

There are many instances of unsteady flows in which analytic solutions, even approximate ones, are not available. This is particularly true of free surface flows when, for example, non-linear waves or even slightly complicated boundaries are involved. Though analytical methods are progressing, especially through the use of variational principles (Whitham [1965]) and, in some cases, the non-linear shallow water wave equations yield important results (Carrier and Greenspan [1958]) there is still a need for numerical methods. Indeed, numerical "experiments" can be used to complement actual experiments.

Until very recently numerical solutions in two dimensions

invariably seemed to employ the Eulerian description of the motion though the Lagrangian concept has been used for some time in the much simpler one-dimensional case (e.g., Heitner [1969], Brode [1969]) and to make small time expansions (Pohle [1952]). Perhaps the best known of these Eulerian methods is the Marker-and-Cell technique (MAC) begun by Fromm and Harlow [1963] and further refined by Welch, et al. [1966], Hirt [1968], Amsden and Harlow [1970], Chan, Street and Strelkoff [1969] and others. The most difficult problem arises in attempting to reconcile the initially unknown shape and position of a free surface with a finite difference scheme and the necessity of determining derivatives at that surface. In the same way, few solutions exist with curved or irregular solid boundaries. In steady flows, mapping techniques have been employed to transform the free surface to a known position (e.g., Brennen [1969]). It would therefore seem useful to examine the use of parametric planes for unsteady flows. The Lagrangian description in its most general form (Lamb [1932]) involves such a plane and by suitable choice of the reference coordinates, the free surface can be reduced to a known and fixed straight line. However a discussion of other parametric planes and mapping techniques is included in Section 3.

The major part of this paper is devoted to the development of a numerical method for the solution of the Lagrangian equations of motion in which full use is made of the flexibility allowed in the choice of reference coordinates. For the moment, we have restricted ourselves to cases of inviscid flow. Very recently, Hirt, Cook and Butler [1970] published details of a method which employs a Lagrangian tagging space but is otherwise similar to the MAC technique. This is further discussed in Section 4B.

## II. LAGRANGIAN EQUATIONS OF MOTION

The general inviscid dynamical equations of motion in Lagrangian form are (Lamb [1932]):

$$(X_{tt}-F)\begin{Bmatrix} X_a \\ X_b \\ X_c \end{Bmatrix} + (Y_{tt}-G)\begin{Bmatrix} Y_a \\ Y_b \\ Y_c \end{Bmatrix} + (Z_{tt}-H)\begin{Bmatrix} Z_a \\ Z_b \\ Z_c \end{Bmatrix} + \frac{1}{\rho}\begin{Bmatrix} P_a \\ P_b \\ P_c \end{Bmatrix} = 0 \qquad (1)$$

where $X, Y, Z$ are the Cartesian coordinates of a fluid particle at time $t$, $F$, $G$, $H$ are the components of extraneous force acting upon it, $P$ is the pressure, $\rho$ the density and $a$, $b$, $c$ are any three quantities which serve to identify the particle and which vary continuously from one particle to the next. For ease of reference $(X,Y,Z)$ are termed Eulerian coordinates, $(a,b,c)$ Lagrangian coordinates. Suffices $a, b, c, t$ denote differentiation.

If $X_0$, $Y_0$, $Z_0$ is the position of a particle at some reference time $t_0$ (when the density is $\rho_0$) then the equation of continuity is simply

$$\rho \frac{\partial(X,Y,Z)}{\partial(a,b,c)} = \rho_0 \frac{\partial(X_0,Y_0,Z_0)}{\partial(a,b,c)} . \qquad (2)$$

Frequently it is convenient to define a, b, c as identical to $X_0$, $Y_0$, $Z_0$, thus reducing the R.H.S. of (2) to $\rho_0$; however it will be seen in the following sections that flexibility in the definition of a, b, c is of considerable value when designing numerical methods of solution.

If the extraneous forces, F, G, H, have a potential $\Omega$ and $\rho$, if not uniform, is a function only of P then, eliminating $\Omega + P/\rho$ from (1):

$$\frac{\partial}{\partial t}(U_bX_c - U_cX_b + V_bY_c - V_cY_b + W_bZ_c - W_cZ_b) = \frac{\partial \Gamma_1}{\partial t} = 0$$

$$\frac{\partial}{\partial t}(U_cX_a - U_aX_c + V_cY_a - V_aY_c + W_aZ_a - U_aZ_c) = \frac{\partial \Gamma_2}{\partial t} = 0 \qquad (3)$$

$$\frac{\partial}{\partial t}(U_aX_b - U_bX_a + V_aY_b - V_bY_a + W_aZ_b - W_bZ_a) = \frac{\partial \Gamma_3}{\partial t} = 0$$

where, for convenience, the velocities $X_t$, $Y_t$, $Z_t$ are denoted by U, V, W. The quantities $\Gamma_1$, $\Gamma_2$, $\Gamma_3$ are related to the Eulerian vorticity components, $\zeta_1$, $\zeta_2$, $\zeta_3$ by

$$\Gamma_1 = \zeta_1(Y_bZ_c - Y_cZ_b) + \zeta_2(Z_bX_c - Z_cX_b) + \zeta_3(X_bY_c - X_cY_b)$$

$$\Gamma_2 = \zeta_1(Y_cZ_a - Y_aZ_c) + \zeta_2(Z_cX_a - Z_aX_c) + \zeta_3(X_cY_a - X_aY_c) \qquad (4)$$

$$\Gamma_3 = \zeta_1(Y_aZ_b - Y_bZ_a) + \zeta_2(Z_aX_b - Z_bX_a) + \zeta_3(X_aY_b - X_bY_a)$$

(Thus, of course, vorticity changes with time are due solely to changes in the coefficients of the L.H.S. of (4) which, in turn, represents stretching and twisting of the vortex line.) Given the vorticity distribution $\zeta(X,Y,Z)$ at some initial time, $t_0$, $\Gamma(a,b,c)$ (which is independent of time) may be obtained through Eqs. (4) and used in the final form of the dynamical equations of motion, namely Eqs. (3) integrated with respect to time.

For incompressible, planar flow the equations reduce to

Continuity: $$X_a Y_b - Y_a X_b = F(a,b) \tag{5}$$

(or differentiated w.r.t. t):

$$U_b Y_a - U_a Y_b + V_a X_b - V_b X_a = 0 \tag{6}$$

Motion: $$U_b X_a - U_a X_b + V_b Y_a - V_a Y_b = -\Gamma(a,b). \tag{7}$$

By introducing the vectors $Z = X + iY$ and $W = U - iV$, (6) and (7) conveniently combine to:

$$Z_a W_b - Z_b W_a = -\Gamma(a,b). \tag{8}$$

Other types of flow have also been investigated. For example, in the case of a heterogeneous, or non-dispersive stratified liquid in which $\rho$ is a function of (a,b), Eq. (8) becomes:

$$Z_a W_b - Z_b W_a = -[\Gamma(a,b)]_{t=t_o} - \frac{1}{\rho}\int_{t_o}^{t} (X_{tt} - F)(\rho_b X_a - \rho_a X_b) + (Y_{tt} - G)(\rho_b Y_a - \rho_a Y_b)\ dt. \tag{9}$$

The integral term therefore manufactures vorticity. The methods developed for a homogeneous fluid in Sections 4A to D are modified in Section 4E to include such effects.

## III. OTHER PARAMETRIC PLANES

It may be of interest to digress at this point to consider other parametric planes (a,b), which are not necessarily Lagrangian. That is to say the restrictions $X_t(a,b,t) = U$, $Y_t(a,b,t) = V$ are abandoned so that U,V are no longer either Eulerian or Lagrangian velocities. Provided $J = \partial(X,Y)/\partial(a,b) \neq 0$, or $\infty$, the equation for incompressible and irrotational planar flow remains

$$Z_a W_b - Z_b W_a = 0. \tag{10}$$

To incorporate one of the advantages of the Lagrangian system, it is required that the free surface be fixed and known, say on a line of constant b. Then the kinematic and dynamic free surface conditions are respectively

$$(U - X_t)Y_a - (V - Y_t)X_a = 0 \tag{11}$$

$$(U_t + F)X_a + (V_t + G)Y_a + (U - X_t)U_a - (V - Y_t)V_a = 0. \tag{12}$$

Now a useful choice concerning the (a,b) plane would be to require the mapping from (X,Y) to be conformal. Then, of course, (10) simply reduces to the Cauchy-Riemann conditions $U_a = -V_b$, $U_b = V_a$ so that $W = U - iV$ is an analytic function of $c = a + ib$ or of $Z$.

In this way, John [1953] has constructed some special, exact analytic solutions. The kinematic condition, (11), has the particular solution $W(a,t) = \overline{Z_t(a,t)}$ on the free surface, which implies $W(c,t) = \overline{Z_t(\bar{c},t)}$ by analytic continuation. If, in addition,

$$Z_{tt} + (F + iG) = iZ_c K(c,t) \tag{13}$$

where K is real on the free surface, then the dynamic condition thereon is also satisfied. John discusses several examples for various choices of the function K.

The potential of such methods may not have been fully realized either analytically or numerically. In the latter case, however, the conformality of the (X,Y) to (a,b) mapping is not necessarily a great advantage, whereas a fixed and known free surface position most certainly is.

The digression ends here and the following sections develop a Lagrangian numerical method from the equations of Section 2.

## IV. A NUMERICAL METHOD EMPLOYING LAGRANGIAN COORDINATES

A method for the numerical solution of incompressible, planar flows is now described. It attempts to take full advantage of the flexibility in the choice of Lagrangian coordinates.

### A. Time Variant Part

The method uses an implicit scheme with central differencing over time, t. Thus $Z^p(a,b)$ is determined at a series of stations in time, distinguished by the integer, p. Knowledge of velocity values, $Z_t^{p+1/2}$, at a midway station $p + \frac{1}{2}$ enables $Z^{p+1}(a,b)$ to be found from $Z^p$ through the numerical approximation

$$Z^{p+1} = Z^p + \tau Z_t^{p+1/2} \quad \text{(error order } \tau^3 Z_{ttt}) \tag{14}$$

where $\tau$ is the time interval. Acceleration values, $Z_{tt}^{p}$, needed in the free surface condition (Section 4C) are approximated by $(Z_t^{p+1/2} - Z_t^{p-1/2})/\tau$ (error order $\tau^4 Z_{tttt}$). Thus the main part of the solution involves finding $P_t^{p+1/2}$ knowing $Z^p$, $Z_t^{p-1/2}$ and their previous values.

The first time step (from $p = 0$ to $p = 1$) requires a little special attention. Clearly $Z^0(a,b)$ is chosen to fit the required initial conditions. But further information is required on a free surface which will enable the accelerations in that condition to be found (see Section 4C).

## B. Spatial Solution

A method of the present type is restricted to a finite body of fluid, S. However, S, could be part of a larger or infinite mass of fluid if an "outer" approximate solution of sufficient accuracy was available to provide the necessary matching boundary conditions at the interface. The region, S, need not be fixed in time. It would indeed be desirable, for example, to "follow" a bore.

In a great number of cases of widely different physical geometry including all the examples of Section 6, it is convenient to choose S to be rectangular in the (a,b) plane. This rectangle (ABCD, Fig. 1) is then divided into a set of elemental rectangles. The motion of each of these cells of fluid is to be followed by determining the Z values at all the nodes.

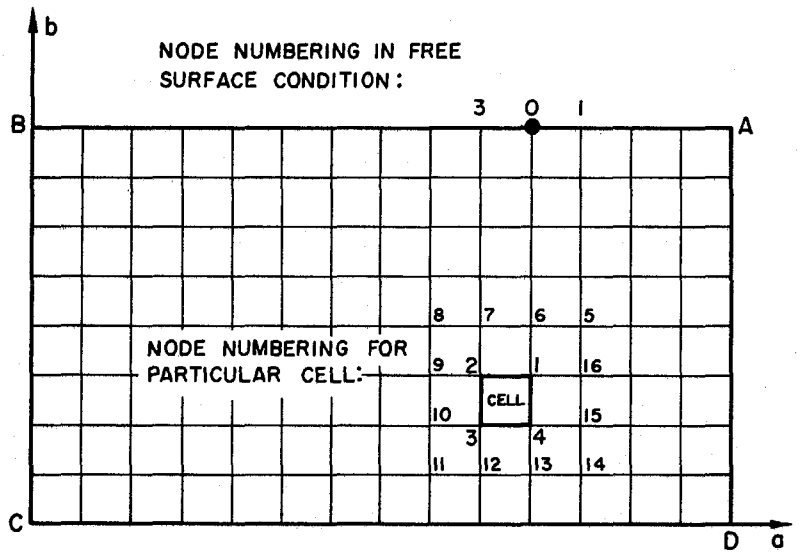


Fig. 1. The Rectangular Lagrangian Space, S, Showing the Numbering Conventions Used

Making the assumption of straight sides the actual area of a cell in the physical plane is

$$A = \tfrac{1}{2}[(X_1 - X_3)(Y_2 - Y_4) - (X_2 - X_4)(Y_1 - Y_3)] \qquad (15)$$

Number suffices refer to the four vertices, numbered anticlockwise; other node numbering conventions are shown in Fig. 1. If this area is to remain unaltered after proceeding in time from station p to p + 1 through Eq. (14) then

$$\text{Imag}\{(Z_2 - Z_4)^p(W_1 - W_3)^{p+1/2} - (Z_1 - Z_3)^p(W_2 - W_4)^{p+1/2}\}$$
$$+ \tau\{(U_1 - U_3)(V_2 - V_4) - (U_2 - U_4)(V_1 - V_3)\}^{p+1/2} + \frac{2(A^p - A^0)}{\tau}$$
$$= 0 = R_c \qquad (16)$$

where the terms on the L.H.S., second line are numerical corrections required to preserve continuity more exactly and prevent accumulation of error over a large number of time steps. The numerical value of the L.H.S. at some point in the iterative solution is termed the continuity residual, $R_c$.

Assuming linear variation in velocity along each side of the cell, evaluating the circulation around 1234 and setting this equal to the known, initial circulation, $\Gamma_c$, yields (in the case of a homogeneous fluid):

$$\text{Real}\{(Z_2 - Z_4)(W_1 - W_3) - (Z_1 - Z_3)(W_2 - W_4)\} - 2\Gamma_c = 0 = R_I \qquad (17)$$

Slight hesitation is required here since, for validity, the Z and W values in this equation should relate to the same station in time. But by choosing to apply it at the midway stations and substituting $Z^{p+1/2} = Z^p + (\tau/2)Z_t^{p+1/2}$ the $\tau$ terms are found to cancel and (17) persists when the values referred to are $Z^p$ and $W^{p+1/2}$. $R_I$ is the circulation residual. The modification of (17) in the case of a heterogeneous fluid is delayed until section 4E.

Combining (16) and (17) produces the cell equation:

$$(Z_2 - Z_4)(W_1 - W_3) - (Z_1 - Z_3)(W_2 - W_4) \qquad \text{Main Part}$$
$$+ i\tau\{(U_1 - U_3)(V_2 - V_4) - (U_2 - U_4)(V_1 - V_3)\} + \frac{2(A^p - A^0)i}{\tau} \qquad \text{Continuity Corrections}$$
$$- 2\Gamma_c \qquad \text{Permanent Cell Circulation Term}$$

$$+ \frac{1}{12}\{(W_{16} + W_9 - W_1 - W_2)(Z_1 - Z_2) \qquad \text{Higher}$$

$$- (W_{15} + W_{10} - W_3 - W_4)(Z_4 - Z_3) \qquad \text{Order}$$

$$+ (W_7 + W_{12} - W_2 - W_3)(Z_2 - Z_3) \qquad \text{Correction}$$

$$- (W_6 + W_{13} - W_1 - W_4)(Z_1 - Z_4)\} \qquad \text{if required}$$

$$= 0 = R_I + iR_c = R, \text{ the cell residual.} \qquad (18)$$

The higher order correction, included for completeness, allows the shape of the cell sides and the variations in velocity along them to be of cubic form. Without it the neglected terms are of order $Z_a W_{bbb}$, $Z_{ab} W_{ab}$, etc., with it they are of order $Z_a W_{bbbbb}$, etc. Values referred to are $Z^p$ and $W^{p+1/2}, U^{p+1/2}, V^{p+1/2}$.

Though this derivation of the cell equation is instructive, it can be obtained more directly (except for the continuity correction) by integration of (8) over the area of the cell in the (a,b) plane (using Taylor expansions about the center of the cell).

The cell equations must now be solved for $W^{p+1/2} = (U - iV)$, $Z^p$ being known, in order to proceed in time.

In a recently published paper, Hirt, Cook and Butler [1970] take a rather different approach in which the (a,b) plane is employed merely as a tagging space. The equations are written in essentially Eulerian terms, no derivatives with respect to a,b appearing. The numerical method (LINC) is similar to that of the MAC technique (Fromm and Harlow [1963], Welch, et al. [1966], Chan, Street and Strelkoff [1969], etc.) and involves solving for the pressure at the center of a cell as well as for the vertex velocities. Advantages of the method described in the present paper are: the pressure has been eliminated (though this may be disadvantageous in compressible flows); no special treatment is required for cells adjacent to boundaries; inhomogeneous density terms are relatively easily included. However, since the LINC system is based on the Eulerian equations of motion, the inclusion of viscous terms is more easily accomplished than in the present method where such an attempt leads to horrendous difficulties.

C. Boundary Conditions

To complete the specifications, a condition upon $W^{p+1/2}$ is required at each of the boundary nodes. This usually takes the form of an expression connecting $U^{p+1/2}$ and $V^{p+1/2}$. For example, solid boundaries, whether fixed or moving in time, may be prescribed by a function, $F(X,Y,t) = 0$. Then the required relation is

$$F(X^p + \tau U^{p+1/2}, Y^p + \tau V^{p+1/2}, t) = 0 \tag{19}$$

Dynamic free surface conditions are simply constructed from Eqs. (1). If, for example, the only extraneous force is that due to gravity, g, in the negative Y direction, the condition on a free surface such as AB, Fig. 1, is

$$X_{tt}X_a + (Y_{tt} + g)Y_a = \frac{T}{\rho}\frac{\partial}{\partial a}\left(\frac{Y_{aa}X_a - X_{aa}Y_a}{(X_a^2 + Y_a^2)^{3/2}}\right) \tag{20}$$

where T is the surface tension if this is required.

Unlike the field Eqs. (8) or (18) these boundary conditions may not be homogeneous in all the variables. In a given problem only the boundary conditions are altered by different choices of typical length, h (perhaps an initial water depth), and typical time, say $\sqrt{h/g}$ in the above example. Then, using the same letters for the dimensionless variables, g and $T/\rho$ in Eq. (20) would be replaced by 1 and $S = T/\rho g h^2$. The numerical form of that condition used at a free surface node such as 0 (Fig. 1) is:

$$(X_1 - X_3)^p(U_0^{p+1/2} - U_0^{p-1/2}) + (Y_1 - Y_3)^p(V_0^{p+1/2} - V_0^{p-1/2} + \tau)$$

$$= \tau S(P_1^p - P_3^p) \tag{21}$$

where P is assessed at each node as

$$P_0 = \frac{[(X_1 - X_3)(Y_1 + Y_3 - 2Y_0) - (Y_1 - Y_3)(X_1 + X_3 - 2X_0)]}{[(X_1 - X_3)^2 + (Y_1 - Y_3)^2]^{3/2}}$$

and the accelerations have been replaced by the expressions given in Section 4A. Again, Eq. (21) relates $U_0^{p+1/2}$ to $V_0^{p+1/2}$ since all other quantities are known.

If the liquid starts from rest at $t = 0$ (as in the examples of Section 6) then difficulties at the singular point $t = 0$ can be avoided by choosing to apply the condition at $t = \tau/4$ rather than $t = 0$. Using $Z_{tt} = 2Z_t^{1/2}/\tau$ and $Z = Z^0 + (\tau/4)Z_t^{1/2}$ at that station the special boundary condition becomes

$$U_0^{1/2}\{(X_1 - X_3)^0 + \frac{\tau}{4}(U_1 - U_3)^{1/2}\} + \frac{\tau}{4}(V_1 - V_3)^{1/2}(V_0^{1/2} + \tau g/2) = 0 \tag{22}$$

in the case of zero surface tension.

D. Method of Solution

It remains to discuss how the equations may be solved to find $W^{p+1/2}$ at every node. Due to the non-linear terms in (18) and some boundary conditions as well as to the fact that a good estimate of $W^{p+1/2}$ can be made from values at previous time stations, a simple iterative or relaxation scheme was employed. Such a method involves visiting each cell in turn and adjusting the W values at its vertices in such a way that repetition of the process reduces the cell residuals, R, to negligible proportions. But, on arrival at a particular cell, there are an infinite number of ways in which its four vertex values can be altered in order to dissipate the single cell residual. However, experience demonstrated that a procedure based on the following changes ($\Delta W_{1,2,3 \text{ and } 4}$) was superior in convergence and stability to any of the others tested:

$$\Delta W_1 = -\Delta W_3 = \omega i R(\overline{Z_1 - Z_3})/8A$$

$$\Delta W_2 = -\Delta W_4 = \omega i R(\overline{Z_2 - Z_4})/8A \qquad (23)$$

Here $\omega$ is an overrelaxation factor and A is the area of the cell, which is unchanged with time and given by the expression (15). These incremental changes have a simple and meaningful physical interpretation. As can be seen from Fig. 2, they are a combination of two changes, one representing pure stretching and the other pure rotation, which dissipate respectively the continuity and circulation components of the residual.

Having visited each and every cell, the boundary conditions were then imposed. Where these were given in the form $A.U^{p+1/2} + B.V^{p+1/2} + C = 0 = R_B$, A,B,C being constants and $R_B$ the residual, the following changes were made, the choice being based upon experience:

$$\begin{Bmatrix} \Delta U^{p+1/2} \\ \Delta V^{p+1/2} \end{Bmatrix} = - \begin{Bmatrix} A \\ B \end{Bmatrix} \frac{R_B}{(A^2 + B^2)} \qquad (24)$$

The whole process was then repeated to convergence.

E. Inhomogeneous Fluid

In a non-dispersive, inhomogeneous fluid, $\rho(a,b)$, which is independent of time, will be prescribed through the initial choice of $Z^0(a,b)$. Indeed in many cases it will be convenient to choose $Z^0$ in

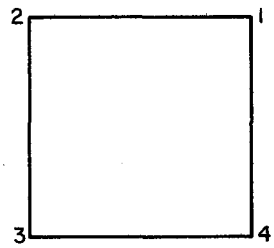


Fig. 2(a). The Cell in the Reference Plane (a,b)

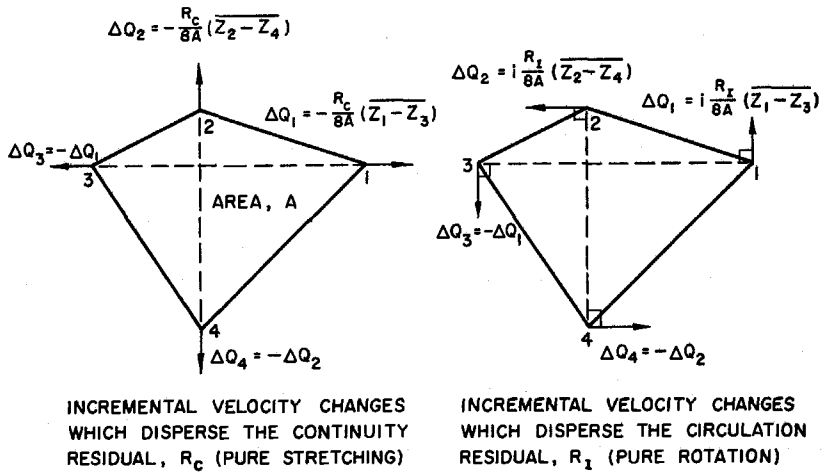


Fig. 2(b). The Cell in the Physical Plane (X,Y)

such a way that $\rho$ is some simple analytic function of (a,b). This is particularly desirable because by substituting for $\rho$, $\rho_a$, $\rho_b$ in Eq. (9), this can then be integrated over a cell area (as in Section 4B) to produce a convenient additional term, $\theta^{p+1/2}$, on the L.H.S. of the cell Eq. (18). Since the expression for $\theta^{p+1/2}$ will depend upon that choice of $\rho(a,b)$ an example will illustrate this.

If $\rho$ is to be constant along the free surface, AB, Fig. 1, and along the bed, CD, it may be possible to choose $Z^o$ such that $\rho$ is a linear function of b, say $\rho = \rho_{CD}(1 + \gamma b)$ where $\gamma = \rho_{AB}/\rho_{CD} - 1$ and $b = 1$ on AB. Then,

$$\theta_{1234}^{p+1/2} - \theta_{1234}^{p-1/2}$$

$$\approx -\frac{1}{4}\ln(1-\mu)\Big[\{(U_1+U_2+U_3+U_4)^{p+1/2} - (U_1+U_2+U_3+U_4)^{p-1/2}\}$$

$$\times \{X_1 - X_2 - X_3 + X_4\}^p$$

$$+\{V_1+V_2+V_3+V_4)^{p+1/2} - (V_1+V_2+V_3+V_4)^{p-1/2} + 4\pi g\}\{Y_1 - Y_2 - Y_3 + Y_4\}^p\Big]$$

$$+\{1 + \frac{1}{\mu} - \frac{1}{2}\ln(1-\mu)\}\Big[(X_1 - X_2)^p\{(U_1+U_2)^{p+1/2} - (U_1+U_2)^{p-1/2}\}$$

$$- (X_4 - X_3)^p\{(U_3+U_4)^{p+1/2} - (U_3+U_4)^{p-1/2}\}$$

$$+ (Y_1 - Y_2)^p\{(V_1+V_2)^{p+1/2} - (V_1-V_2)^{p-1/2} + 2\tau g\}$$

$$- (Y_4 - Y_3)^p\{(V_3+V_4)^{p+1/2} - (V_3+V_4)^{p-1/2} + 2\tau g\}\Big]$$

where $\mu = \gamma\Delta b/(1+\gamma b_{34})$, $b_{34}$ being the b value on side 34 of the cell and $\Delta b$ the difference across each and every cell. The first term is of order $\mu$, the second order $\mu^2$. The boundary conditions are usually identical to the homogeneous case.

## V. ACCURACY, STABILITY, CONVERGENCE AND SINGULARITIES

### A. Accuracy

If the cell equation, (18), is used without the higher order spatial correction, an indication of the errors due to neglected higher order spatial derivatives can be obtained by assessing the value of that correction and inferring its effect upon the final values of W. Unfortunately, the mesh distribution and mesh size required for a solution of given accuracy will not be known a priori and can only be arrived at either by trial and error or by using some technique of rezoning. The latter method in which cells are subdivided where and when the violence of the motion demands it, can be difficult to program satisfactorily and has not been attempted thus far.

Errors due to higher order temporal derivatives are most easily regulated by ensuring that, for each cell, both $\tau|W_1 - W_3|/|Z_1 - Z_3|$ and $\tau|W_2 - W_4|/|Z_2 - Z_4|$ are comfortably less than unity. A workable rule of thumb can be devised in which a suitable $\tau$ for a particular time step is determined from the W and Z values of the preceding step.

B. Stability of Cell Relaxation

Suppose the central member, cell A, of the group of cells shown in Fig. 3 contained a residual $R_A$ which was then dissipated according to the relations (23). Transfer functions, $D_{AB}$, $D_{AC}$, etc., will describe the residual changes, $\Delta R_B$, etc., in the surrounding cells where

$$\Delta R_B = \omega D_{AB} R_A, \text{ etc.} \tag{24}$$

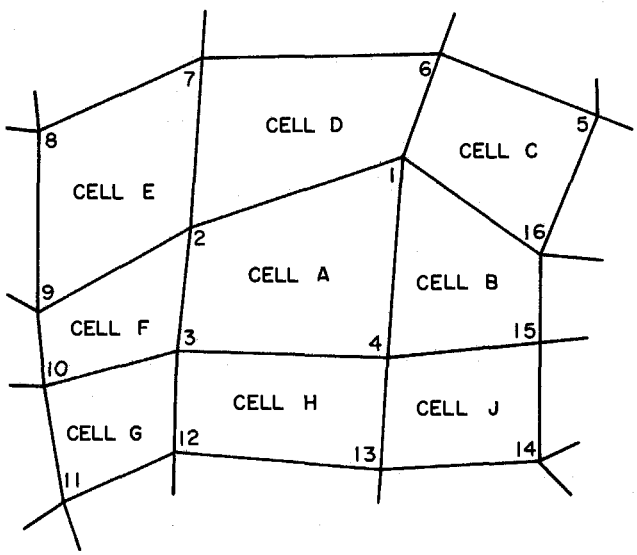


Fig. 3. Z-Plane

For example

$$D_{AB} = \{(Z_1 - Z_{15})(Z_2 - Z_4) - (Z_{16} - Z_4)(Z_1 - Z_3)\}i/8A_A$$

where $A_A$ is the area of cell A. For convergence of the relaxation method it is clearly necessary that the $\omega$ for each cell be chosen so that all $\omega|D|$ are significantly less than unity. It is instructive to inspect the case in which all the cells are roughly geometrically similar in the Z plane. Then

$$|D_{AB}| = |D_{AD}| = |D_{AF}| = |D_{AH}| \approx \frac{|d_1^2 - d_2^2|}{8A_A} = \gamma_1$$

$$|D_{AC}| = |D_{AE}| = |D_{AG}| = |D_{AJ}| \approx \frac{d_1 d_2}{8A_A} = \frac{1}{4} + \gamma 2$$

where $d_1$, $d_2$ are the lengths of the cell diagonals. For square cells, $\gamma_1 = \gamma_2 = 0$ and the situation is stable. However difficulties may arise when the cells are very skewed or elongated and it is in such situations, in general, that care has to be taken with the relaxation technique.

C. Observation on the Cell Equation

One feature of the basic cell equation, (18), itself demands attention. Note that without the higher order spatial correction, the residuals, R in all of the cells (of Fig. 3) remain unaltered when the W or Z values at alternating points (say the odd numbered points of Fig. 3) are changed by the same amount. Such alternating "errors" must be suppressed. Some damping is provided by the higher order spatial correction since it is not insensitive to these changes. But experience showed this to be insufficient unless all the boundary conditions also inhibited such alternating "errors." Solid boundaries usually provide adquate damping. For instance, in Fig. 4(a) fluctuations in U on BC, DA and in V on BC are obviously barred. But the free surface provides little or no such suppression and as will be seen in the next section this can lead to difficulties. It is of interest to note that some of the solutions of Hirt, Cook and Butler [1970] exhibit the same kind of alternating errors.

In the MAC technique, neglected higher order derivatives of the diffusion type and with negative coefficients (a "numerical" viscosity) can lead to a numerical instability if not counteracted by the introduction of sufficient real viscosity. In the present method, as with that of Hirt, Cook and Butler [1970], the convection terms which cause that problem are not present. The higher order spatial correction does contain terms of diffusion order, but it cannot be directly correlated with a viscosity since viscous terms are of a different form (i.e., like $\int \nu \nabla^2_{xy} \Gamma \, dt$). Also, the higher order spatial correction has a beneficial rather than a destabilizing effect.

D. The Free Surface

By including previously neglected derivatives, the numerical free surface condition (without surface tension) is found to correspond more precisely to:

$$\{X_a X_{tt} + Y_a(Y_{tt} + 1)\} + \frac{(\Delta a)^2}{6}\{X_{aaa} X_{tt} + Y_{aaa}(Y_{tt} + 1)\}$$

$$+ \frac{\tau^2}{24}\{X_a X_{tttt} + Y_a Y_{tttt}\} = 0 \qquad (26)$$

where $\Delta a$ is the a difference across a cell and the second and third terms constitute truncation errors. Inspect this in the light of a linearized standing wave solution (see Section 6A), i.e.,

$$X = a - M \cos \sqrt{k}\, t \sin ka\, e^{kb}$$

$$Y = b + M \cos \sqrt{k}\, t \cos ka\, e^{kb}$$

where the variables are non-dimensionalized as in Section 4C and k is the non-dimensional wave number in the a,b plane. Then, the second and third terms of Eq. (26) will be insignificant provided

$$\frac{k^2(\Delta a)^2}{6} \ll 1 \quad \text{and} \quad \frac{\tau^2 k}{24} \ll 1$$

respectively. Or, in terms of a wavelength, $\lambda = 2\pi/k$:

$$\frac{\lambda}{\Delta a} \gg 2 \quad \text{and} \quad \tau \ll 4 \frac{\lambda}{\Delta a} \Delta X \tag{27}$$

since $\Delta a \approx \Delta X$, the X difference between points on the free surface. The first condition states the inevitable; namely, that the solution will be hopelessly inaccurate for (a,b) plane wavelengths comparable with the mesh-length $\Delta a$. Given that the first condition holds then the second says that $\tau \ll 8\Delta X$. For a travelling wave system the same condition states that $\tau$ should be less than the time taken for a wave to travel one mesh length. This constitutes a restriction on $\tau$ which is usually more stringent than that of Section 5A. If, for example, the depth of the fluid is divided into N intervals and the X difference across each cell is of the same order as the Y difference then $\tau$ should be less than $8/N$.

A more difficult problem arises when the first condition is considered alongside the fact, ascertained in the previous section, that the field equation provides little or no resistance to disturbances whose wavelength is equal to $\Delta a$. The only resort would seem to be to some artificial damping technique which would eliminate or suppress these small wavelengths. The technique used in the examples to follow was to relax the W values on the free surface such that $W = \beta W^{FSC} + (1 - \beta) W^*$ where $W^{FSC}$ was the value indicated by the free surface condition, $W^*$ the value which would make the numerical equivalent of $W_{aaaa}$ be zero at that point and $\beta$ was slightly less than one half.

## E. Singularities

Successful numerical treatments of singularities depend upon the availability of analytic solutions to the flow in the neighborhood of that point. For example, at a corner between solid walls the velocity varies as the $(\pi - \beta)/\beta$ power of distance from that junction where $\beta$ is the included angle. If this is $\pi/2$ (as at points C or D, Fig. 4(a)) the variation is linear and thus the numerical estimate of the circulation around the cell (see Section 4) in such a corner is a good one. Where the angle is not $\pi/2$ (D, Fig. 4(c)) errors will occur due to the non-linear variation of velocity, but corrective procedures are easily devised.

A great deal less is known about the singularities at a junction of a free surface and a solid boundary. If the wall is static and vertical (A, Fig. 4(a)) so that $X_{tt} = X_b = X_{bt} = 0$, etc., it follows from the equation of motion that if $Y_a = 0$ at $t = 0$ then it is always zero for irrotational flow; the tangent to the free surface at the wall is always horizontal. Thus the free surface condition without surface tension is automatically satisfied at such a junction and only weak singular behavior is expected. But a similar analysis of the case when the wall begins to move at $t = 0$ (remaining vertical) indicates that $Y_{tt}$ must be infinite at the junction (B, Fig. 4(a)) at $t = 0$, the singularity being logarithmic in space. An extension to $t \neq 0$ has not so far been obtained. One approach might be a Fourier analysis of the step in $X_{tt}$ so that the steadily oscillating solutions of Fontanet [1961] could be used. These suggest that $Y_{tt}$ becomes finite for $t > 0$.

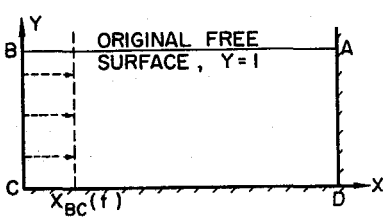


FIG. 4(a)

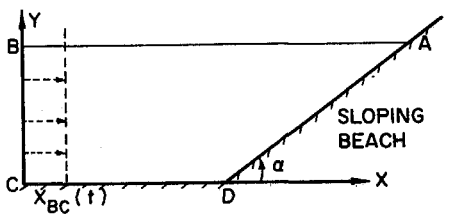


FIG. 4(c)

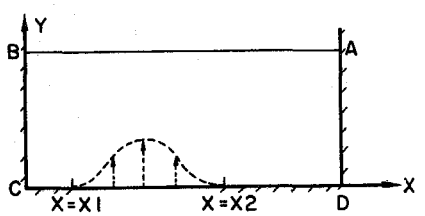


FIG. 4(b)

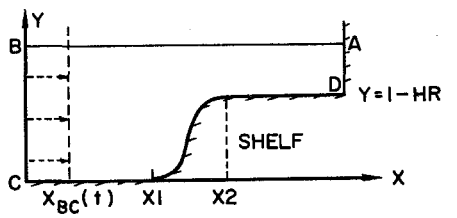


FIG. 4(d)

In the examples to follow (see Figs. 4(a) to (d)) satisfactory numerical solutions could be obtained by ignoring all but one of the singularities. The exception was the shoreline, point A, Fig. 4(c). If $\beta$ is the angle between the tangent to the free surface at A and the horizontal then correlating the two boundary conditions yields:

$$(Z_{tt})_A = - e^{i\alpha}/(\cot \beta \cos \alpha + \sin \alpha) \qquad (28)$$

Thus the sign of $\beta$ determines the direction of the acceleration up or down the beach. If the fluid starts from rest at $t = 0$, $\beta = 0$, then $(Z_{tt})_{t=0} = 0$ and successive differentiation of the basic equation (8) and the boundary conditions yields (for irrotational motion):

At A, $t = 0$ $(\alpha \neq \frac{\pi}{2})$ $\qquad Z_{tt}, Z_{ttt} = 0$

$$Z_{tttt}, Z_{att}, Z_{btt}, Z_{ttttt} = 0 \text{ or } \infty, \text{ unless } \alpha = \frac{\pi}{4} \qquad (29)$$

$$Z_{tttttt}, Z_{attt}, Z_{bttt} = 0 \text{ or } \infty, \text{ unless } \alpha = \frac{\pi}{4} \text{ or } \frac{\pi}{6}$$

These relations suggest a behavior which is logarithmically singular in time at $t = 0$ unless $\alpha = \pi/2n$, n integer. Roseau [1958] found similar logarithmic singularities in periodic solutions for the general case which excluded $\alpha = \pi/2n$ and another set of particular angles (see also Lewy [1946]). But a systematic analysis of the singular behavior (especially for $t \neq 0$) has not as yet been completed. Rather, since the relations (29) no longer necessarily hold if the condition of irrotationality near that point is relaxed, the problem was circumvented numerically by replacing the circulation condition on the single cell in that corner by the condition (28) at the point A and the time $t = 0$ was avoided by applying (28) at $t = \tau/4$ just as was done with the general free surface condition (Section 4C).

Note that strong singularities could be introduced by unsuitable mapping to the (a,b) plane.

## VI. SOME RESULTS INCLUDING COMPARISONS WITH LINEAR SOLUTIONS

### A. Lagrangian Linearized Solutions

Linearized solutions to the Lagrangian equations are obtained by substituting $X = a + \xi$, $Y = B + \eta$ into the equations of continuity and motion and neglecting all multiples of derivatives of $\xi$ and $\eta$. For incompressible and irrotational planar flow the Cauchy-Riemann conditions $\xi_a = - \eta_b$, $\xi_b = \eta_a$ result so that $\xi + i\eta$, and therefore $Z - c$ (where $c = a + ib$) is an analytic function of $\overline{c}$. In the absence

of surface tension the free surface condition reduces to

$$\xi_{tt} + g\eta_a = 0 \qquad (g = 1 \text{ in the dimensionless variables}) \qquad (30)$$

only when the additional assumption that $\eta_{tt} \ll g$ is made. In this way harmonic solutions can be obtained for some simple problems.

In passing, it may be of interest to compare Lagrangian linearization with the more common Eulerian type, at least in some simple cases. For travelling waves on an infinite ocean the first order Lagrangian terms are precisely those of Gerstner's waves. The Eulerian solution must be taken to the third order to achieve this waveform. On the other hand, while the Eulerian solution is always irrotational the Lagrangian only approaches it. Thus the comparitive accuracy of the two methods depends upon what particular feature of the flow is under scrutiny. A comparison of the works of Zen'kovich [1947] and Penney and Price [1952] for standing waves on an infinite ocean demonstrates the same features.

B. Example One, Figs. 4(a), 5, 6, 7, 8, 9, and 10

In the example of Fig. 4(a), the liquid is initially at rest in the rectangular vessel BCDA; between $t = 0$ and $t = T$ the side BC moves inward according to

$$X_{BC}(t) = M \sin^2 \pi t/2T \qquad \text{for} \qquad 0 < t < T$$

$$= M \qquad \text{for} \qquad t > T$$

With a suitable choice of M and T this creates a wave which travels along the box, builds up on and is reflected by the opposite wall, AD. The linearized solution (which requires a Fourier analysis of the free surface boundary condition) is

$$Z - c = X_{BC}(t)\left[1 - \frac{\bar{c}}{\ell}\right] + \sum_{k=1}^{\infty} R_k B_k(t) \sin\left(\frac{k\pi\bar{c}}{\ell}\right) \qquad (31)$$

where

$$R_k = M/\pi k \left(\frac{\nu k^2 T^2}{\pi^2} - 1\right) \cosh\left(\frac{\pi k}{\ell}\right)$$

$$B_k(t) = \cos \nu_k t - \cos \frac{\pi t}{T}, \qquad 0 < t < T$$

$$= \cos \nu_k t + \cos \nu_k (t - T), \qquad t > T$$

$$\nu_k = \left[\frac{k\pi}{\ell} \tanh \frac{k\pi}{\ell}\right]^{\frac{1}{2}}$$

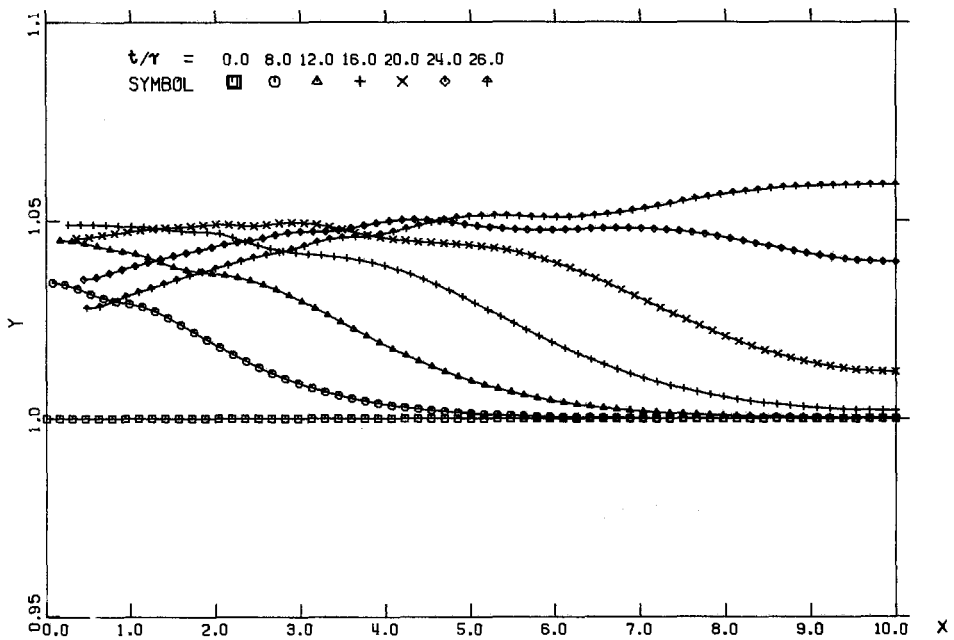


Fig. 5. Linearized solution to example 1: $M = 0.53$, $T = 32\tau$, $\tau = 0.53$, showing free surface position at a selection of times, t.

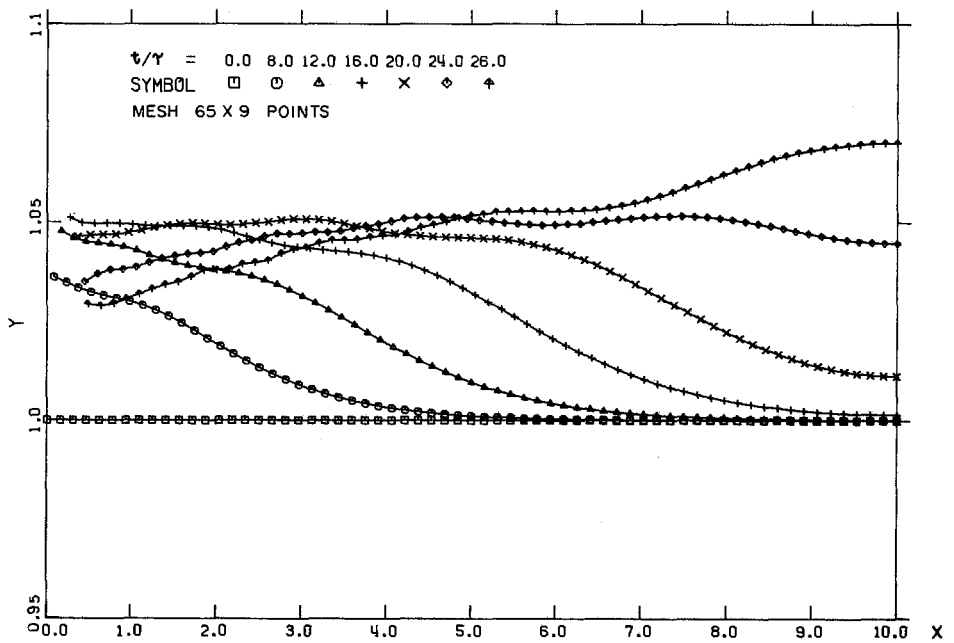


Fig. 6. Numerical solution to example 1: $M = 0.53$, $T = 32\tau$, $\tau = 0.53$, showing free surface position at a selection of times, t

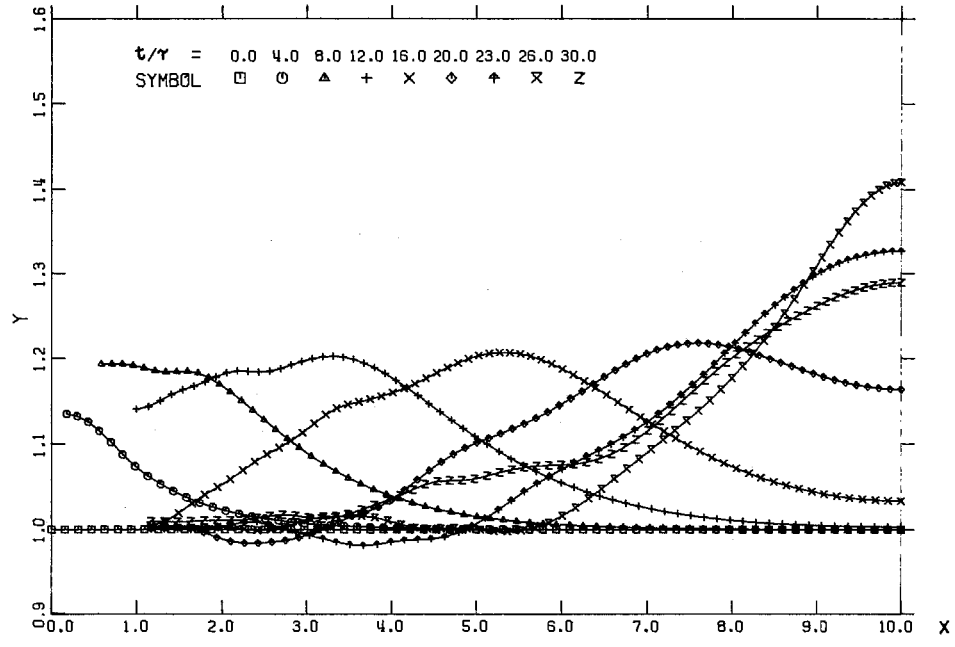


Fig. 7. Linearized solution to example 1: M = 1.16, T = 16$\tau$, $\tau$ = 0.60, showing free surface position at a selection of times, t

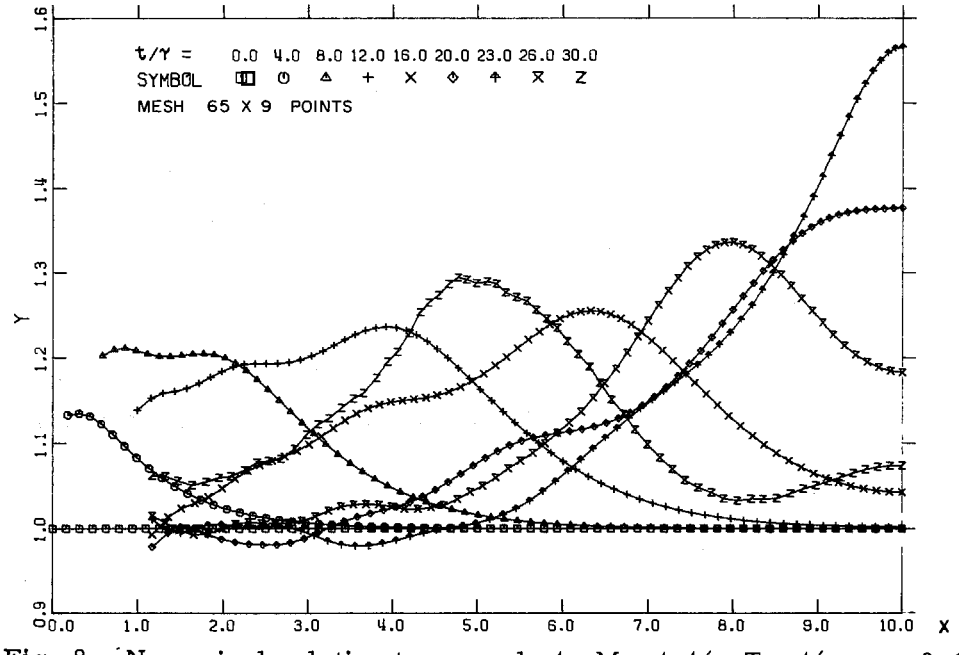


Fig. 8. Numerical solution to example 1: M = 1.16, T = 16$\tau$, $\tau$ = 0.60, showing free surface position at a selection of times, t

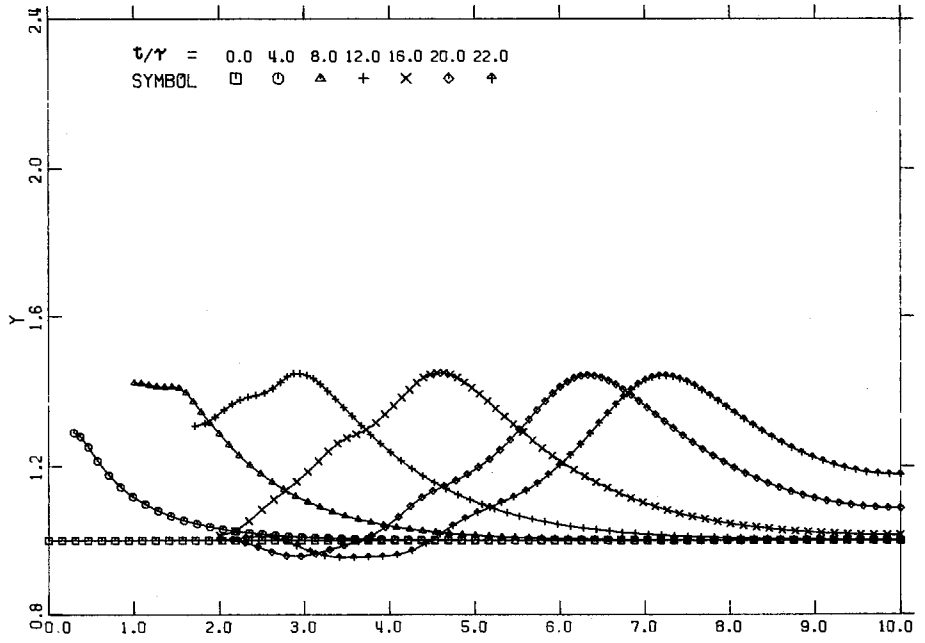


Fig. 9. Linearized solution to example 1: $M = 2.00$, $T = 16\tau$, $\tau = 0.48$, showing free surface position at a selection of times, t

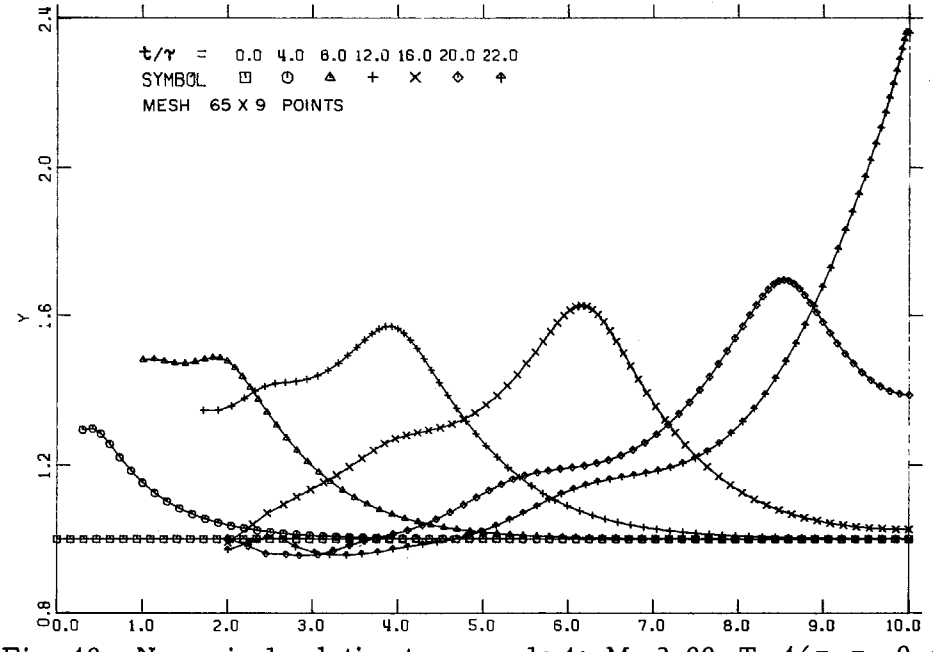


Fig. 10. Numerical solution to example 1: $M = 2.00$, $T = 16\tau$, $\tau = 0.48$, showing free surface position at a selection of times, t

and $\ell$ is the a difference between the walls AD and BC. In Figs. 5 and 6, 7 and 8, 9 and 10 the numerical and linearized free surface shapes are compared for three cases of increasing wave amplitude. As the amplitude increases the similarity between the two diverges; both the wave velocity and the build up on the wall become progressively greater in the numerical solution. Note also that, especially in Fig. 10, the peak of the wave is much sharper than in the linearized solution. For amplitudes less than that of Figs. 5 and 6 the results were almost identical.

C. Example Two, Figs. 4(b), 11, and 12

The second example, Fig. 4(b), introduces moving and curved solid boundaries; the liquid is disturbed from rest by a bed uplift of the form:

$$\text{For } X1 < X < X2,\ Y_{CD} = M \sin^2\left[\frac{\pi t}{2T}\right] \sin^2\left[\frac{\pi(X - X1)}{(X2 - X1)}\right] \quad \text{for } 0 < t < T$$

$$= M \sin^2\left[\frac{\pi(X - X1)}{(X2 - X1)}\right] \quad \text{for } t > T$$

$$\text{For } X < X1,\ X > X2, \quad Y_{CD} = 0 \quad \text{all } t$$

Within certain extreme limits on M and T this causes a surface wave immediately above the bed disturbance which then spreads out to each side and is followed by a depression wave over the bed uplift. The linearized solution is

$$Z - c = \frac{iM}{4} \cdot \frac{(X2 - X1)}{\ell} \cdot A(t) + \sum_{k=1}^{\infty} R_k \left[ i \tanh\left(\frac{\pi k}{\ell}\right) A(t) \cos\left(\frac{k\pi\bar{c}}{\ell}\right) + B_k(t) \sin\left(\frac{k\pi\bar{c}}{\ell}\right)\right] \tag{32}$$

where

$$R_k = M\left\{\sin\left(\frac{k\pi X2}{\ell}\right) - \sin\left(\frac{k\pi X1}{\ell}\right)\right\} \Big/ 2\ell\nu_k^2\left\{1 - \left(\frac{k(X2 - X1)}{2\ell}\right)^2\right\}$$

$$\nu_k = \left[\frac{k\pi}{\ell} \tanh \frac{k\pi}{\ell}\right]^{\frac{1}{2}}$$

$$A(K) = 2 \sin^2 \frac{\pi t}{T} \quad \text{for} \quad 0 < t < T, \quad = 2 \quad \text{for } t > T$$

$$B_k(t) = \sigma_k \cos \nu_k t + 1 - (1 + \sigma_k) \cos \frac{\pi t}{T} \quad \text{for} \quad 0 < t < T$$

$$= 2 + \sigma_k(\cos \nu_k t + \cos \nu_k(t - T) \quad \text{for} \quad t > T$$

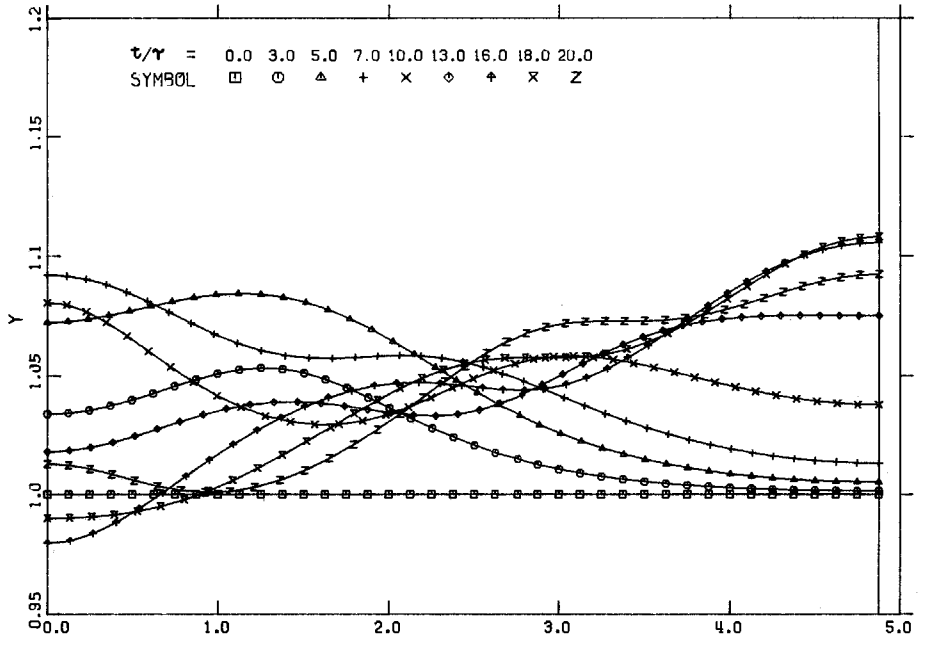


Fig. 11. Linearized solution to example 2: M = 0.344, X1 = 0.75, X2 = 2.12, T = 6τ, τ = 0.35, free surface positions at selection of times, t

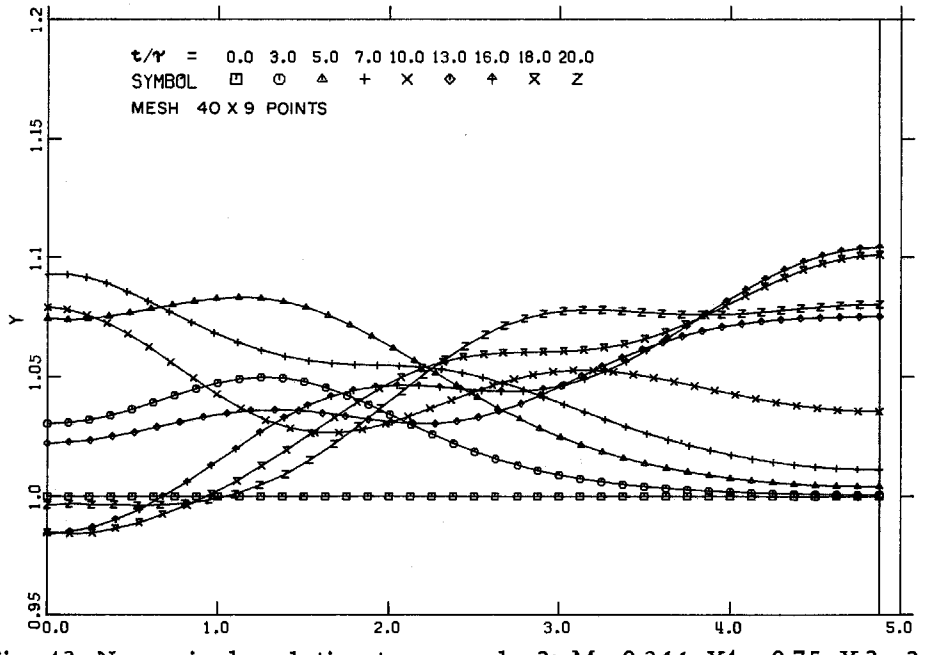


Fig. 12. Numerical solution to example 2: M = 0.344, X1 = 0.75, X 2 = 2.12, T = 6τ, τ = 0.35, free surface positions at selection of times, t

$$\sigma_k = \operatorname{sech}^2\left(\frac{\pi k}{\ell}\right) \Big/ \left[\frac{T^2 \nu_k^2}{\pi^2} - 1\right]$$

and $\ell$ is the a difference between the vertical walls. For T of the order of 2 or 3 and for values of M up to 0.3, at least, there was virtually no difference between the numerical and linearized solutions. Figures 10 and 11 in which M = 0.344 demonstrate this.

D. Example Three, Figs. 4(c), 13, 14, 15. A Sloping Beach

By altering the condition on the boundary AB of example one and employing the shoreline treatment of Section 5E, the interaction of the waves with a sloping beach could be studied. In Fig. 13 a small wave appraches a 27° beach. As the horizontal inclination of the tangent to the free surface at the shoreline ($\beta$) decreases, the shoreline (A) accelerates up the beach until $\beta$ becomes positive. The acceleration then reverses (as in Eq. (28)) and the wave reaches maximum run up. The backwash is extremely rapid and positions $t/\tau$ = 21, 22 suggest that this causes the small wave which is following the main one to break. By this time the cells have become very distorted and the mesh points excessively widely spaced to allow further progress. A similar succession of events takes place with the larger wave and smaller beach angle (18°) of Fig. 14. Note in this case the large run-up to wave-height ratio. In neither of these cases does there appear to be any tendency for the main wave to break on its approach run. Indeed the reaction with the beach is similar to the behavior predicted by Carrier and Greenspan [1958] in their non-linear shallow water wave analysis. The wave amplitude was further increased and the beach slope decreased to 9° in an attempt to produce breaking on the approach run. A preliminary result is shown in Fig. 15. Variations in the application of the free surface condition and in the shoreline treatment have, as yet, failed to remove the irregularities in that solution. A stronger shoreline singularity coupled with an insufficiently rigorous treatment of it may be to blame. An optimistic viewer might detect a breaking tendency.

E. Example Four, Figs. 4(d), 16. A Shelf

One final example is shown in Figs. 4(d) and 16 where the wave travels up a shelf, created by changing the boundary condition on CD, Fig. 1. Excessive vertical elongation of the cells on top of the shelf caused this computation to be stopped at the last time shown. (At this point the wave height/water depth ratio on the shelf is of the order of 2.) However, one can detect a splitting of the wave into two waves as might be expected from the theory of Lax [1968].

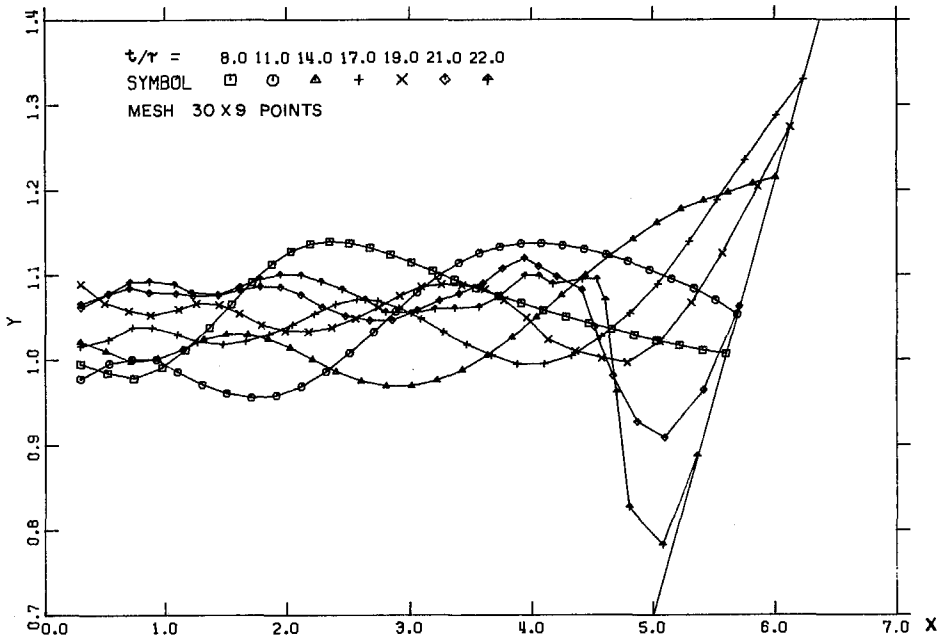


Fig. 13. Example 3 with $M = 0.30$ and $T = 6\tau$, $\tau = 0.571$. The beach slope is $27^{\circ}$. Free surface positions at selection of times, t

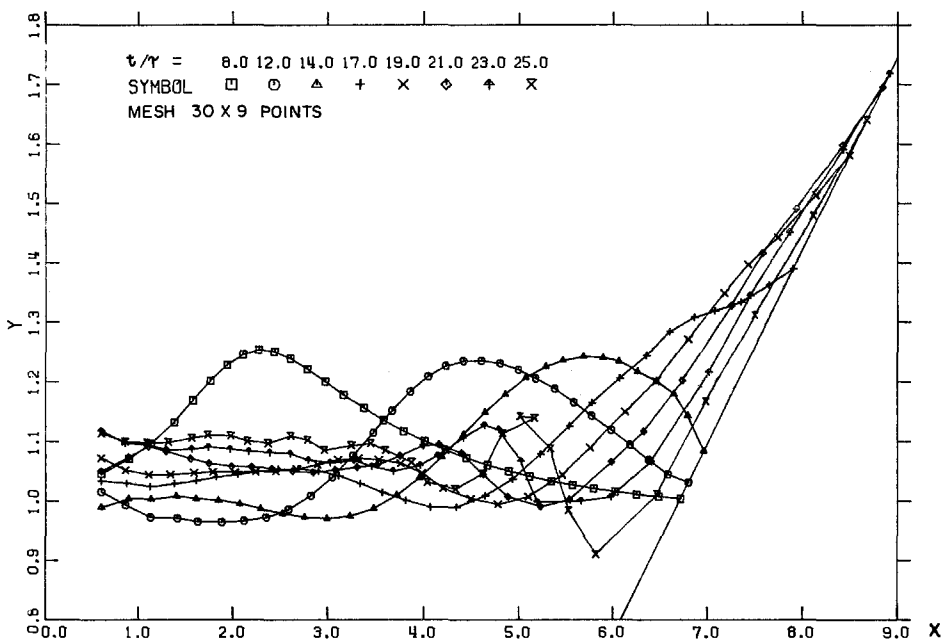


Fig. 14. Example 3 with $M = 0.60$ and $T = 8\tau$, $\tau = 0.571$. The beach slope is $18^{\circ}$. Free surface positions at selection of times, t

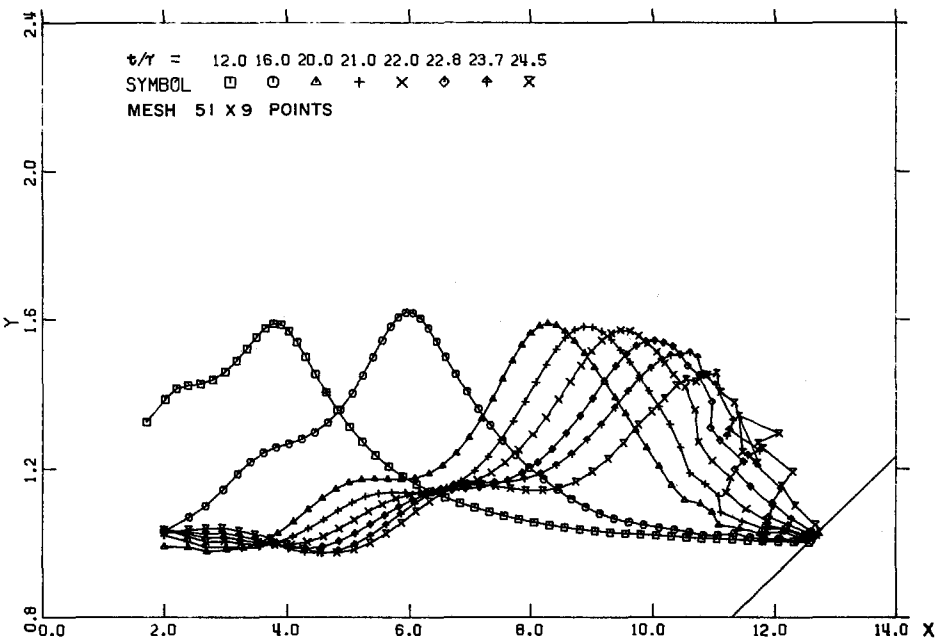


Fig. 15. Example 3 with M = 2.00, T = 16$\tau$, $\tau$ = 0.481. The beach slope is 9°. Free surface positions at selection of times, t

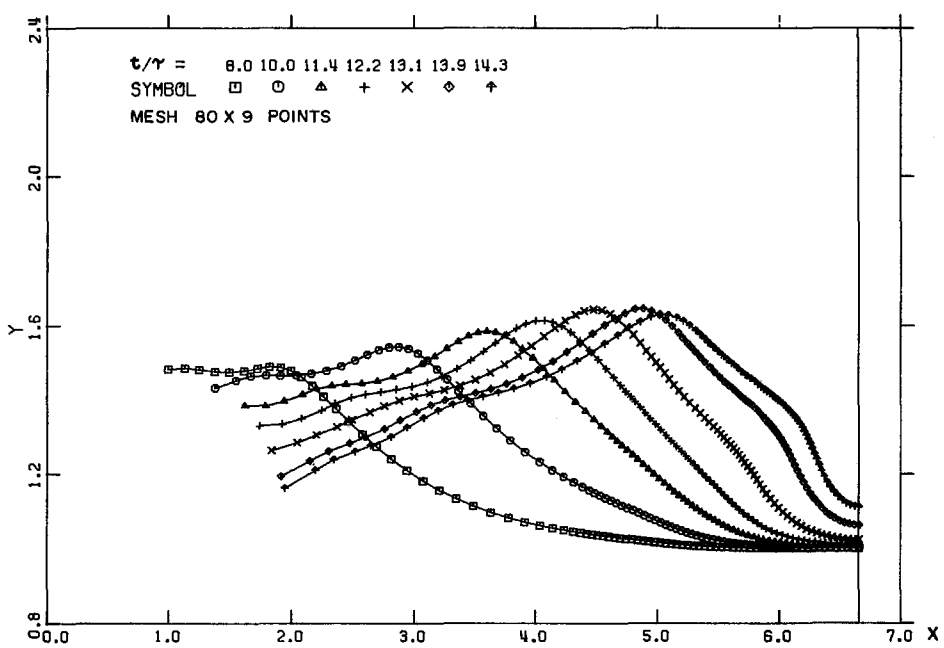


Fig. 16. Example 4 with M = 2.00, T = 16$\tau$, $\tau$ = 0.481. Shelf defined by X1 = 4.41, X2 = 5.16, HR = 0.3. Free surface positions at selection of times, t

## VII. CONCLUDING REMARKS

Rather severe examples were taken in order to test the limiting characteristics of the method developed. Provided the various interval limitations were adhered to only two problems arose which could prematurely conclude a computation. First, excessive elongation of the cells in regions of the most violent motion could cause the mesh points to be excessively widely spaced; rezoning could, however, make it possible to continue. Secondly, it would appear that a more detailed knowledge and treatment of some singularities is required. Work on this, and especially on the shoreline singularity of example three, is in progress at the moment.

Other types of examples which have been only briefly investigated thus far are: the matching with a semi-infinite region in which some analytic solution is used; the inclusion of surface tension; the extension of the method to three dimensions; examples in which the fluid is inhomogeneous. It is hoped to present such results in the near future.

The authors are deeply appreciative of the kind and considerate help given by Professor T. Y. Wu.

This work was partially sponsored by the National Science Foundation under grant GK 2370 and by the Office of Naval Research under contract N00014-67-A-0094-0012.

## REFERENCES

Amsden, A. A. and Harlow, F. H., The S.MAC method: A numerical technique for calculating incompressible fluid flows, Los Alamos Scientific Laboratory Report LA-4370, 1970.

Biesel, F., "Study of wave propagation in water of gradually varying depth," in Gravity Waves, U.S. National Bureau of Standards NBS Circular 521, 1952.

Brennen, C., "A numerical solution of axisymmetric cavity flows," J. Fluid Mech., 37, 4, 1969.

Brode, H. L., "Gas dynamic motion with radiation: a general numerical method," Astronautica Acta, 14, 1969.

Carrier, G. F. and Greenspan, H. P., "Water waves of finite amplitude on a sloping beach," J. Fluid Mech., 4, 1958.

Chan, R. K-C., Street, R. L. and Strelkoff, T., Computer studies of finite amplitude water waves, Stanford University Civil Engineering Technical Report No. 104, 1969.

Fontanet, P., Théorie de la génération de la houle cylindrique par un batteau plan, Thesis, University of Grenoble, 1961.

Fromm, J. E. and Harlow, F. H., "Numerical solution of the problem of vortex street development," Physics of Fluids, 6, 1963.

Heitner, K. L., A mathematical model for the calculation of the run-up of tsunamis, Thesis, California Institute of Technology, 1969.

Hirt, C. W., The numerical simulation of viscous incompressible fluid flows, Proceedings of the 7th ONR Symposium, Rome, 1968.

Hirt, C. W., Cook, J. L. and Butler, T. D., "A Lagrangian method for calculating the dynamics of an incompressible fluid with free surface," J. of Computational Physics, 5, 1970.

John, F., "Two-dimensional potential flows with free boundaries," Communs. Pure and Appl. Math, 6, 1953.

Lamb, H., Hydrodynamics (6th Ed.), Cambridge University Press, 1932.

Lax, P. D., "Integrals of non-linear equations of evolution and solitary waves," Communs. Pure and Appl. Math., 21, 1968.

Lewy, H., "Water waves on sloping beaches," Bull. Amer. Math. Soc., 52, 1946.

Penney, W. G. and Price, A. T., "Finite periodic stationary gravity waves in a perfect liquid," Phil. Trans. Roy. Soc., A, 244, 1952.

Pohle, F., "Motions of water due to breaking of a dam, and related problems," in Gravity Waves, U.S. National Bureau of Standards Circular 521, 1952.

Roseau, M., "Short waves parallel to the shore over a sloping beach," Communs. Pure and Appl. Math., 11, 1958.

Sekerz-Zen'kovich, Ya. I., "On the theory of standing waves of finite amplitude on the surface of a heavy fluid," (R) Dokl. Akad. Nauk. SSSR, (N.S.), 58, 1947.

Wehausen, J. V. and Laitone, E. V., "Surface Waves," Handbuch der Physik, Vol. IX, Fluid Dynamics III, 1960.

Welch, J. E., Harlow, F. H., Shannon, J. P. and Daly, B. J. The MAC method, Los Alamos Scientific Laboratory Report No. LA-3425, 1966.

Whitham, G. B., "A general approach to linear and non-linear dispersive waves using a Lagrangian," J. Fluid Mech., 22, 2, 1965.